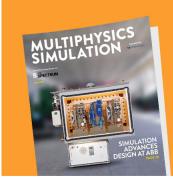# Development of high quantum efficiency GaAs/GaInP double heterostructures for laser cooling

Daniel A. Bender, Jeffrey G. Cederberg, Chengao Wang, and Mansoor Sheik-Bahae

Development of high quantum efficiency GaAs/GaInP double heterostructures for laser cooling

Daniel A. Bender,[1,a)] Jeffrey G. Cederberg,[1] Chengao Wang,[2] and Mansoor Sheik-Bahae[2]

[1]*Sandia National Laboratory, P.O. Box 5800, Albuquerque, New Mexico 87185, USA*
[2]*Department of Physics and Astronomy, University of New Mexico, 800 Yale Blvd. NE, Albuquerque, New Mexico 87131, USA*

We report on the growth and characterization of high external quantum efficiency (EQE) GaAs/GaInP double heterostructures. By properly treating the GaAs/GaInP interface, we are able to produce structures measuring a record EQE of 99.5% ± 0.1% in GaAs. This efficiency exceeds the requirement for achieving laser cooling in GaAs. However, net cooling has not yet been realized due to residual below gap background absorption. © 2013 AIP Publishing LLC.
[http://dx.doi.org/10.1063/1.4811759]

External quantum efficiency (EQE) can be effectively described as the probability that the recombination of an electron-hole pair gives rise to a luminescence photon escaping into the free space. This quantity plays an important role in assessing the operation of many photonic devices such as lasers, light-emitting diodes, and photovoltaics.[1] An emerging application that has the most stringent requirement on high EQE materials is optical refrigeration or laser cooling in solids.[2,3] Motivated by the latter, we have investigated the growth of extremely high EQE GaAs-based structures. A semiconductor based optical cooler offers the attraction of direct integration with focal plane array sensor layers as well as superconducting electronics. For a given injected electron-hole density (N), EQE (η_{eqe}) in an intrinsic semiconductor can be expressed as[2,4]

$$\eta_{eqe} = \frac{\eta_e B N^2}{AN + \eta_e B N^2 + C N^3},\qquad(1)$$

where A, B, and C are nonradiative, radiative, and Auger recombination coefficients, respectively, and η_e is the luminescence escape efficiency. An optimum density of $N = (A/C)^{1/2}$ maximizes EQE at $\sim 1 - (AC)^{1/2}/2\eta_e B$.

For optical refrigeration to be realized, very high radiative quantum efficiency is needed. Recently, Zhang *et al.* demonstrated optical refrigeration in CdS nano-belts with an estimated EQE > 99%, marking the first demonstration for laser-induced refrigeration in a semiconductor material.[5] In spite of much theoretical[6,7] and experimental[2,4,8] work in GaAs, net cooling has not yet been realized. For GaAs at 100 K the EQE must be greater than 99% to achieve cooling with a background absorption $\alpha_b \leq 0.5$ cm^{-1}.[9] This extreme demand on external quantum efficiency has been approached in the literature with a metal-organic chemical vapor deposition (MOCVD) grown sample achieving 98.8% ± 0.2%,[2] but even with the high EQE cooling was not accomplished due to excessive parasitic background absorption. Other measurements of EQE have been performed on both MOCVD and molecular beam epitaxy (MBE) grown samples which revealed, in general, MBE prepared samples have a lower

background absorption, MOCVD prepared samples produce higher EQE.[10]

High EQE is required for cooling based on anti-Stokes photoluminescence (PL), but there are other processes for which laser cooling could take place. One recent example is anti-Stokes Raman scattering, which is proposed to work with efficiencies of only a few percent in nitride-based materials.[11]

Schnitzer *et al.* measured the EQE of room temperature planar GaAs heterostructures by pumping above the bandgap and collecting the integrated photoluminescence in all specular directions.[12] This signal was referenced to scatter from a white Lambertian surface to calibrate the EQE. They observed an EQE as high as 72% corresponding to an internal quantum efficiency of 99.7% in the GaAs layer. Dunstan pointed out that separate measurement of photoluminescence and a photo-thermal signal for the same excitation conditions can yield the absolute quantum efficiency.[13] This is because the absorbed power must be converted into either light or heat: a fractional increase of one is accompanied by a fractional decrease of the other. This approach can give higher measurement accuracy as EQE approaches unity. Gfroerer *et al.* used this principle to collect luminescence in tandem with sample temperature using a thermistor as a function of excitation power.[14] By normalizing these two fractional quantities to the excitation power and plotting them against each other, the expected linear relationship is observed.

Using a modified form of the above experiment, Catchpole *et al.* measured an EQE of 92% in GaAs passivated with GaInP and mounted on a ZnSe substrate.[15] They showed that modulated pump light can increase sensitivity and reduce complications from long-term thermal drift. Gauck *et al.* attached a similar GaAs/GaInP heterostructure to a ZnSe hemispherical lens to increase luminescence extraction efficiency, resulting in an EQE of 96% at the optimum excitation level.[4]

The extremely high mobility in GaAs/AlGaAs double heterostructures (DHS) grown by MBE were shown to exhibit low EQE and are not suitable for optical refrigeration.[16] The GaAs/GaInP structure can be grown lattice matched and sufficiently high PL lifetimes have been observed to suggest they are a better candidate among III–V materials for laser cooling demonstration.[17]

a)Electronic mail: dabende@sandia.gov

The fabrication of GaAs/InGaP DHS by MOCVD is not new, but laser cooling these heterostructures is a challenging task and represents a worthwhile test of the materials and the synthesis technique. To prepare GaAs/InGaP DHS, we utilized low-pressure MOCVD at 60 Torr. Trimethyl gallium (TMGa) and trimethyl indium (TMIn) were combined with arsine or phosphine in a vertical high-speed rotating disk (1000 rpm) chamber. Two different TMGa sources allowed the GaAs growth rate to be varied independently of the need to achieve a lattice-matched GaInP composition. The temperature was controlled at 650 °C using emissivity correcting pyrometry. For GaAs, a growth rate of 20 nm/min was achieved with 25 μmol/min at a V/III ratio of 50. For GaInP, a growth rate of 35 nm/min was obtained with 35 μmol/min of TMGa and 26 μmol/min of TMIn at a V/III = 160. We found the best surface morphology was obtained with GaAs (100) with a 6° miscut toward a (111)A direction. This substrate specification was used for all samples evaluated in this study. Growth was initiated by depositing a 50 nm AlAs layer, for use in subsequent epitaxial lift off, followed by 700 nm of GaInP, 700 nm of GaAs, and 700 nm of GaInP. The wafer was cooled to 300 °C before the PH_3 flow was terminated. The GaInP barriers were doped with silicon to a level of 2×10^{17} cm^{-3}, while the GaAs layer was not intentionally doped with an n-type background of 1×10^{15} cm^{-3}.

Our initial experimental efforts deposited GaAs and GaInP heterostructure continuously, without particular attention to the chemical differences between compounds. This growth sequence is illustrated in Figure 1(a). The reality is much more complex. Chemical exchange leads to unintended composition grading over short distances between these two compounds.[18–20] We observed this dramatically as significant compressive strain in what should be lattice matched superlattice structures. To avoid this grading a thin GaP layer was inserted between the inverted interface, going from GaInP to GaAs as illustrated in Figure 1(b).[21,22] GaP is under significant tensile strain grown on GaAs or lattice matched GaInP so only very thin layers can be used. We grew nominally 0.6 nm, but did not attempt to characterize this thickness. This insertion eliminated the compressive stress observed in the GaAs/GaInP superlattices. The only interface we impacted was the inverted one; the regular GaAs to GaInP interface was grown continuously without any adjustment. This is in contrast to other reports that perform treatments on both interfaces.[23,24] We speculate that the inverted interface undergoes significant intermixing on

the anion sub-lattice and indium segregation, while the regular interface is well ordered.[25]

We initially screen and characterize our MOCVD-grown GaAs/GaInP double-heterostructures by temporally and spectrally resolved PL emission. A CW diode laser operating at 785 nm is routed through a fiber optic illuminating the sample. Photoluminescence is collected through the same fiber which is bifurcated sending a fraction of the collected PL to a scanning monochromator for spectral detection. Figure 2(a) illustrates the results of the spectral characterization for the growth conditions detailed in Figure 1. Room temperature PL from sample 2 exhibits a much smoother spectrum below the band edge, Fig. 2(a) (black line). In contrast, PL from sample 1, Fig. 2(a) (red line), shows an extended pedestal below the gap arising from the lack of an intermediate GaP layer on the inverted GaAs/GaInP interface. The existence of this pedestal indicates the presence of states not associated with bulk GaAs.

In a second series of measurements, we use a pulsed laser diode ($\lambda = 785$ nm, 58 ps duration and 5.5 pJ per pulse) operating at 25 kHz to illuminate the GaAs layer. A collection fiber is placed in front of the sample and off axis relative to the excitation laser to avoid collection of reflected laser light. Gathered PL emitting from the opposite end of the

FIG. 2. (a) PL spectra collected from samples with the growth conditions of Fig. 1. The pronounced pedestal of sample 1 (red line) indicates states below the bandgap arising from the lack of an intermediate GaP layer. (b) PL lifetimes for the two samples in (a). Measured data (solid lines) and single exponential fits (dashed lines) show a large difference in nonradiative lifetime.
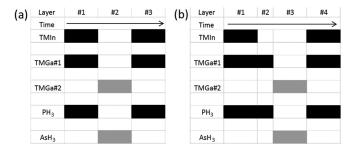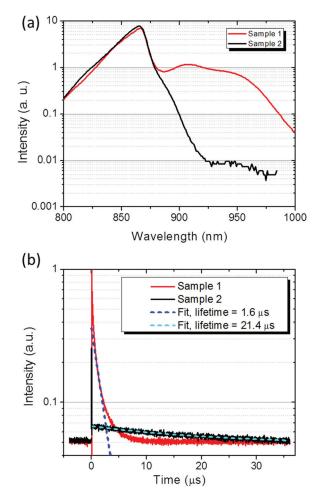
FIG. 1. Illustrations of the growth sequences used for (a) sample 1 and (b) sample 2. In (b), we introduced a thin GaP layer between the lower barrier and the active GaAs layer. The time dimension is not drawn to scale for clarity.

collection fiber is collimated and sent through a 785 nm notch filter to remove any residual laser light and is subsequently detected with a photomultiplier tube (Hamamatsu H10721-20). The time-resolved decay is spectrally integrated and averaged on an oscilloscope. We fit the late-time tail of the photoluminescence decay tail to avoid contribution from Auger and radiative recombination mechanisms present in GaAs at high carrier concentration. Fitting with a single exponential indicates minimal contribution from these nonlinear terms and gives the nonradiative recombination lifetime.[16]

Time resolved PL from samples 1 and 2 is presented in Fig. 2(b) (red and black lines, respectively). With judicious treatment of the inverted GaAs/GaInP interface, nonradiative lifetime in excess of 21 μs can be achieved, Fig. 2(b) (black line). Without an optimized interface, the nonradiative recombination rate increases and lifetimes can drop by more than an order of magnitude. An example of this reduction is observed in Fig. 2(b) (red line).

Based on spectral-temporal PL characterization, sample 2 is a more favorable candidate for laser cooling. Figure 3 shows an All-optical Scanning Laser Calorimetry (ASLC) measurement of the same type and from the same experimental setup detailed in Ref. 10. An ASLC trace depicts the laser-induced temperature change versus the photon energy (wavelength), tuned in the vicinity of the bandgap while keeping the injected carrier density (or luminescence power P_{lum}) constant [see Eq. (2)]. A 1 mm diameter GaAs/GaInP double heterostructure sample is wafer bonded to a 5 mm diameter ZnS hemispheric dome lens and placed in an optical cryostat held at 100 K. Temperature differences produced by the excitation laser are measured by means of non-contact differential luminescence thermometry (DLT). DLT is an all optical, non-contact technique based on a spectral shift in the luminescence resulting from temperature dependence of the bandgap.[10] The minimum resolvable temperature difference for our setup using DLT is <1 mK and is primarily limited by the temperature stability of the cryostat. A temperature change, ΔT, is generated from a pump laser operating at frequency ν and is expressed as[10]
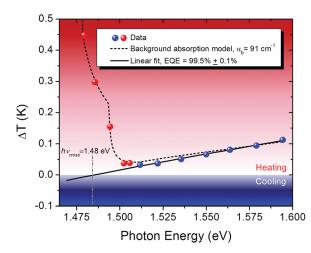

FIG. 3. All-optical scanning laser calorimetry data for GaAs/GaInP DHS performed at 100 K. Each data point is the average of three measurements. Error bars are smaller than the size of the data points. The linear fit (Eq. (2)) gives an EQE of 99.5% (solid line). Long wavelength data (red spheres) is used in fitting the background absorption model using Eq. (5) (dashed line).

$$\Delta T(\nu) = \kappa P_{lum}\left(\frac{\nu}{\tilde{\nu}_f \eta_{eqe}} - 1\right), \qquad (2)$$

where $\tilde{\nu}_f$ is the mean fluorescent frequency, P_{lum} is the escaped luminescence power density, κ is a constant of proportionality dependent on thermal loading. When $\Delta T = 0$, heating exactly balances cooling and the so called zero-crossing condition is met. The photon energy at which this is expected to happen is labeled $h\nu_{cross}$ in Fig. 3. To determine this energy for our sample a linear fit (solid line) is performed to the data represented with blue spheres and extrapolated to $\Delta T = 0$, where $h\nu_{cross} = 1.48$ eV (Fig. 3, gray dotted-dashed line). The EQE is then computed as

$$\eta_{eqe} = \frac{\nu_{cross}}{\tilde{\nu}_f}. \qquad (3)$$

The mean fluorescent energy is obtained through a separate spectral measurement and is taken after the sample has reached thermal equilibrium. The linear fit to data points shown in blue gives a record high EQE of 99.5% $\pm$ 0.1%, Fig. 3 (solid line). We use a separate PL spectrum measurement from which we obtain the resonant (band-edge) absorption spectrum $\alpha_r(\nu)$ using the reciprocity principle.[10] Below the bandgap the resonant absorption falls off rapidly and parasitic background absorption, α_b, becomes non-negligible in its modification of the absorption efficiency

$$\eta_{abs}(\nu) = \frac{\alpha_r(\nu)}{\alpha_r(\nu) + \alpha_b} \qquad (4)$$

and subsequently the induced temperature change

$$\Delta T(\nu) = \kappa P_{lum}\left[\frac{1}{\eta_{eqe}}\frac{\nu}{\tilde{\nu}_f}\left(1 + \frac{\alpha_b}{\alpha_r(\nu)}\right) - 1\right]. \qquad (5)$$

Taking into account the background absorption and the extracted EQE from the high energy data points (Fig. 3, blue spheres), Eq. (5) regressed using a least squares minimization routine to determine a best fit for all data points including low energy data points (Fig. 3, red spheres) by adjusting α_b. For the data in Fig. 3 $\alpha_b = 91$ cm^{-1} and the model of Eq. (5) using the optimized value of background absorption is plotted, Fig. 3 (dashed line). It is important to note that we have assumed the background absorption is constant (i.e., independent of excitation wavelength), which produces a good fit to the data in this case, but in general α_b can be sample specific or geometry dependent. Note the slight deviation in the fit from Eq. (5), indicating minor frequency dependence in the background absorption. We set Eq. (5) equal to zero and solve for the α_b term to yield the maximum tolerable background absorption to reach zero-crossing. Given the EQE of 99.5%, $\alpha_{b_{max}} = 0.19$ cm^{-1} for pumping $k_B T$ below the mean fluorescent energy. These values are in good agreement with the theoretical analysis from Ref. 9. With unity EQE and excitation at $h\nu \approx h\tilde{\nu}_f - k_B T$ the maximum tolerable background absorption to achieve cooling would be 1.44 cm^{-1}, considerably lower than the experimentally determined 91 cm^{-1}.

Through precise control of the growth sequence, improved crystallographic order at the inverted GaAs/GaInP

heterojunction results in high EQE. This improvement in EQE comes via a reduction in interface recombination. Net cooling, however, has not been observed because of residual background absorption in the GaAs/GaInP interface, bulk GaAs layer or bulk passivation GaInP layer. Identifying the source of this absorption is a challenging problem. We have ruled out the bulk GaInP passivation layer as a source of defective states by measuring a sample with a GaInP passivation layer 1/10th the thickness of sample 2 (70 nm). No reduction in background absorption was observed in the ASLC measurement.

Additionally, we cannot find a direct correlation between EQE and background absorption. That is, improving EQE does not necessarily lower background absorption and vice versa. The origin of background absorption in GaAs (in particular) is still unknown. MOCVD GaAs contains carbon impurities that are intrinsic to the metal-organic source used for deposition. While these impurities can be reduced, they cannot be eliminated.[26] Native point defects, such as vacancies or interstitials, represent a more likely source of background absorption.[27] Modification of the growth conditions might lower the background absorption further, but we are uncertain if it can be lowered enough to achieve optical cooling.

[1]O. Miller, E. Yablonovitch, and S. Kurtz, IEEE J. Photovoltaics **2**(3), 303 (2012).
[2]M. Sheik-Bahae and R. I. Epstein, Nat. Photonics **1**, 693 (2007).
[3]M. Sheik-Bahae and R. I. Epstein, Phys. Rev. Lett. **92**, 247403 (2004).
[4]H. Gauck, T. H. Gfroerer, M. J. Renn, E. A. Cornell, and K. A. Bertness, Appl. Phys. A **64**, 143 (1997).
[5]J. Zhang, L. Dehui, R. Chen, and Q. Xiong, Nature **493**, 504 (2013).
[6]J. B. Khurgin, Phys. Rev. Lett. **98**, 177401 (2007).
[7]G. Rupper, N. H. Kwong, and R. Binder, Phys. Rev. B **76**, 245203 (2007).
[8]E. Finkeissen, M. Potemski, P. Wyder, L. Vina, and G. Weimann, Appl. Phys. Lett. **75**, 1258 (1999).
[9]M. Sheik-Bahae and R. I. Epstein, Laser Photonics Rev. **3**, 67 (2009).
[10]C. Wang, C.-Y. Li, M. P. Hasselbeck, B. Imangholi, and M. Sheik-Bahae, J. Appl. Phys. **109**, 093108 (2011).
[11]Y. J. Ding and J. B. Khurgin, Laser Photonics Rev. **6**(5), 660 (2012).
[12]I. Schnitzer, E. Yablonovitch, C. Caneau, and T. Gmitter, Appl. Phys. Lett. **62**, 131 (1993).
[13]D. J. Dunstan, J. Phys. D: Appl. Phys. **25**, 1825 (1992).
[14]T. H. Gfroerer, E. A. Cornell, and M. W. Wanlass, J. Appl. Phys. **84**, 5360 (1998).
[15]K. R. Catchpole, K. L. Lin, P. Campbell, M. A. Green, A. W. Bett, and F. Dimroth, Semicond. Sci. Technol. **19**, 1232 (2004).
[16]B. Imangholi, M. P. Hasselbeck, M. Sheik-Bahae, R. I. Epstein, and S. Kurtz, Appl. Phys. Lett. **86**, 081104 (2005).
[17]J. M. Olson, R. K. Ahrenkiel, D. J. Dunlavy, B. Keyes, and A. E. Kibbler, Appl. Phys. Lett. **55**, 1208 (1989).
[18]R. Bhat, M. A. Koza, M. J. S. P. Brasil, R. E. Nahory, C. J. Palmstrom, and B. J. Wilkens, J. Cryst. Growth **124**, 576 (1992).
[19]T. Nittono, S. Sugitani, and F. Hyuga, J. Appl. Phys. **78**, 5387 (1995).
[20]R. Kudela, M. Kucera, B. Olejnikova, P. Elias, S. Hasenohrl, and J. Novak, J. Cryst. Growth **212**, 21 (2000).
[21]T. K. Sharma, M. R. Gokhale, and B. M. Arora, J. Cryst. Growth **213**, 241 (2000).
[22]X. B. Zhang, J. H. Ryou, R. D. Dupuis, G. Walter, and N. Holonyak, Jr., J. Electron. Mater. **35**, 705 (2006).
[23]R. B. Laghumavarapu, N. Nuntawong, A. R. Albrecht, and D. L. Huffaker, Proc. SPIE **6461**, 64610M (2007).
[24]T. Nakano, T. Shioda, E. Abe, M. Sugiyama, N. Enomoto, Y. Nakano, and Y. Shimogaki, Appl. Phys. Lett. **92**, 112106 (2008).
[25]C. Frigeri, G. Attolini, M. Bosi, C. Pelosi, and F. Germini, J. Electrochem. Soc. **156**, H448 (2009).
[26]T. F. Kuech and E. Veuhoff, J. Cryst. Growth **68**, 148 (1984).
[27]D. T. J. Hurle, J. Appl. Phys. **85**, 6957 (1999).